ACS Sustainable Chemistry & Engineering

pubs.acs.org/journal/ascecg

Research Article

Comparative Life-Cycle Assessment of Biochar and Nickel Catalysts for CO_2-Free Hydrogen Production via Methane Decomposition

Raziyeh Jokar, Hossein Jahromi,* Ashish Manandhar, Sushil Adhikari, Prakash Nepal, Richard Bergman, Naveenkumar Rajendiran, and Ajay Shah

Cite This: *ACS Sustainable Chem. Eng.* 2026, 14, 6083−6098

Read Online

ACCESS | Metrics & More | Article Recommendations | Supporting Information

ABSTRACT: Growing concerns about global warming from fossil fuel combustion underscore the need for sustainable hydrogen production. Catalytic methane decomposition (CMD) offers a CO_2-free pathway by generating hydrogen and solid carbon. This study performs a cradle-to-gate life-cycle assessment of CMD using two catalytic systems, including Ni/Al_2O_3 (metal-based) and biochar (renewable carbon-based), for producing 1 kg H_2 under physical and economic allocation approaches. The physical allocation results demonstrated biochar's superior environmental performance, with 26% lower fossil fuel depletion (11.30 vs 15.32 MJ) and 31% lower global warming impact (3.04 vs 4.38 kg CO_2 eq) compared to Ni catalysts. In contrast, economic allocation results showed smaller improvements for biochar compared to the Ni catalyst (reductions of 17.21 and 25.07% for fossil fuel depletion and global warming impact, respectively). These findings highlight biochar's promise as a sustainable catalyst for CMD and support the broader transition toward low-carbon hydrogen technologies.

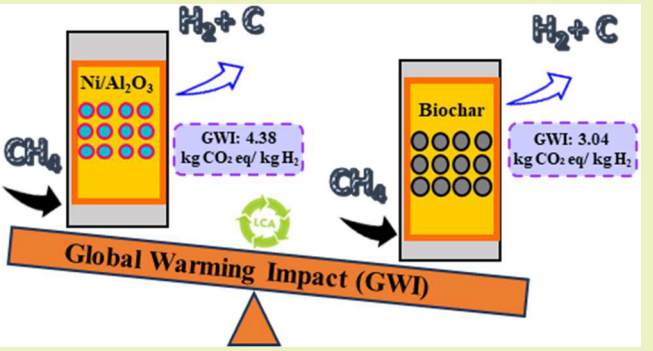

KEYWORDS: *environmental impact, biochar catalyst, nickel catalyst, hydrogen, global warming, carbon, fossil fuel depletion, Process design*

INTRODUCTION

Hydrogen is emerging as a highly efficient and clean energy vector, becoming a center of attention in the pursuit of sustainable energy solutions. The demand for clean energy sources is driving the projected increase in hydrogen production; the global goal is to produce 110 million metric tons (Mt) per year by 2030 and approximately 240 Mt by 2040.[1] According to the International Renewable Energy Agency (IRENA), global hydrogen production amounts to approximately 75 million metric tons of pure hydrogen per year, along with an additional 45 million metric tons produced annually as part of mixed gases. Hydrogen can be produced from both fossil-based and renewable sources. Fossil fuel-based methods primarily include hydrocarbon reforming and pyrolysis, with methane being the most suitable feedstock in this category.[2] Renewable hydrogen production processes, on the other hand, are typically classified according to their reliance on water or biomass as the primary resource.[2] Currently, hydrogen production from methane involves several processes, including steam methane reforming (SMR), dry methane reforming, partial oxidation of methane (POM), autothermal reforming of methane (ATR), and catalytic methane decomposition (CMD).[3]

SMR and POM are efficient and thus cost-effective in hydrogen production, however, they produce significant amounts of carbon oxides (CO_x), and the need for hydrogen purification, often through multiple unit operations, makes the process more complicated and expensive than desired.[4]

Approximately 48% of global hydrogen is produced through the SMR method, which operates with an efficiency of 60−75%.[5] Although generally less expensive than other methods at \$1.5−2.00/kg H_2 SMR generates around 10 kg CO_2/kg H_2 due to the water−gas shift reaction.[5] In contrast, CMD is gaining attention as a promising alternative due to its lower energy requirements, absence of CO_x emissions during the production stage, and production of valuable solid carbon as a coproduct. Keipi et al.,[6] evaluated the economic viability of CMD and reported that the break-even price for carbon produced via CMD is \$0.36/kg in the current market scenario and \$0.33/kg in a projected market scenario for 2030. Above

Received: December 8, 2025
Revised: March 7, 2026
Accepted: March 8, 2026
Published: March 13, 2026

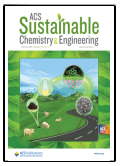

https://doi.org/10.1021/acssuschemeng.5c13361
ACS Sustainable Chem. Eng. 2026, 14, 6083−6098

these values, CMD would be economically competitive with SMR. Although CMD produces less stoichiometric hydrogen per unit mole of methane than SMR, it does not need complex downstream processes. It generates significant amounts of solid carbon, making CMD both environmentally and economically advantageous.[7] Additionally, CMD is attractive considering the current carbon pricing applied to CO_2 emissions from energy-intensive industries, which further enhances its economic viability.[5,8]

Catalysts are crucial in the CMD process and are broadly classified into metal-based and carbon-based types. Fe, Cu, and Ni[[9−11] are the most promising catalysts in the metal catalysts classification. These catalysts exhibit high catalytic activity but face challenges such as rapid deactivation due to carbon deposition, the need for frequent regeneration, and difficulties in separating carbon materials.[12] On the other hand, while carbon-based catalysts are less effective, they offer advantages such as being cheaper and more resistant to impurities and high temperatures. Furthermore, they have cheaper and easier separation methods since they do not contain active metal species. In some instances, separation can be entirely bypassed, allowing the product to be directly used in other processes. Catalyst regeneration is widely considered a solution to deactivation; however, it faces challenges such as secondary emissions and carbon material waste. Studies show that CO_2 and/or CO emissions during regeneration are similar to those from SMR, undermining CMD's environmental benefits and requiring additional hydrogen purification.[13,14] Furthermore, efficiently separating and collecting carbon products without compromising catalyst activity remains a significant technical challenge. From an economic perspective, the cost-effectiveness of CMD heavily depends on the market value of carbon coproducts and methane, highlighting the need for viable industrial applications of carbon materials produced.[13,14]

Given hydrogen's potential as an energy carrier to reduce CO_2 emissions, it is essential to ensure its production performs better environmentally. Life cycle assessment (LCA) is a standardized methodology used to evaluate the environmental impacts of a product throughout its life cycle.[15,16] LCA has been extensively used to assess the sustainability and carbon reduction potential of various hydrogen production pathways. Timmerberg et al.,[17] examined the greenhouse gas (GHG) emissions of various hydrogen production technologies, including three configurations of methane decomposition: plasma, molten metal, and thermal gas. Their findings indicated that the plasma system using renewable energy produced the lowest GHG emissions, at approximately 6 kg CO_2 eq/kg H_2. However, without using renewable energy, the GHG emissions from methane decomposition systems ranged between 11 and 14 kg CO_2 eq/kg H_2. Dufour et al.,[18] conducted a comprehensive LCA of hydrogen production methods from fossil fuels. They concluded that autothermal reforming (2.725 kg CO_2 eq/kg H_2), natural gas decomposition (2.847 kg CO_2 eq/kg H_2), and coal gasification (1.112 kg CO_2 eq/kg H_2) were the most favorable options from multiple perspectives. These lower emissions than expected are the result of considering avoided CO_2 emissions such as from nonproduced electricity. In a separate study, Oni et al.,[19] performed a comparative assessment of hydrogen production methods, considering the impact of plant size and carbon capture extent on cost and life cycle GHG emissions. For a production capacity of 607 tonnes of hydrogen per day, they found that blue hydrogen from autothermal reforming had the lowest life cycle GHG emissions (3.91 kg CO_2 eq/kg H_2), followed by natural gas decomposition (4.54 kg CO_2 eq/kg H_2) and SMR (8.20 kg CO_2 eq/kg H_2). Interestingly, their results also showed that without carbon capture storage (gray hydrogen), natural gas decomposition exhibited lower GHG emissions (4.89 kg CO_2 eq/kg H_2) compared to autothermal reforming (11.01 kg CO_2 eq/kg H_2).

Existing studies have commonly compared various hydrogen production methods, consistently indicating that methane/natural gas decomposition is among the methods with the lowest GHG emissions. Notably, the cross-influence of catalyst type (metal-based vs carbon-based) and reaction conditions (temperature, gas hour space velocity, catalyst lifetime, and regeneration processes) on CMD's environmental footprint has not been thoroughly examined. This study addresses this gap by conducting a comprehensive assessment of CMD using two representative catalysts, nickel and biochar, under varied operating conditions. As CMD technologies are still under development, the findings from this work provide a more realistic and holistic comparison, advancing understanding of CMD's potential for sustainable hydrogen production. The analysis contributes to improved insight into the sustainability and reliability of CMD and offers guidance for optimizing catalytic systems to achieve higher efficiency and better environmental performance. The LCA followed standard procedures, including goal and scope definition, functional unit selection, system boundary determination, life cycle inventory compilation, and impact assessment.

METHODOLOGY

To evaluate the life-cycle environmental impact of the CMD process, an attributional cradle-to-gate life cycle assessment was performed. using free openLCA 2.1.1 software (https://openLCA.org), and the ecoinvent 3.9.1 database (ecoinvent 2021), comparing metal-based and carbon-based catalytic systems in the United States. Using physical allocation, LCA was conducted using a cradle-to-gate system boundary to measure the environmental footprint of a product from extracting raw materials needed up to the point it leaves the factory gate. This means that the environmental impacts assessed do not include the product's use by customers or its end-of-life processes, such as waste management, recycling, or upcycling. Sensitivity analyses were conducted for comparison to the baseline (reference). The following scenarios included using different allocation approaches, use of renewable energy sources, gas hourly space velocity (GHSV), life of catalyst, and no regeneration of the metal catalyst. The cradle-to-gate system boundary was selected for the following reasons: (a) it is the most commonly used system boundary in the materials industry and is consistent with the data sets for conventional reference materials, enabling direct comparisons with different hydrogen production methods, and (b) it represents the system boundary under direct control of the operations involved in the production process. This assessment adhered to ISO 14040 and 14044 standards. The LCA case study was conducted using the tool for the reduction and assessment of chemical and other environmental impacts (TRACI) 2.1 impact assessment methodology developed by the U.S. Environmental Protection Agency.

Goal and Scope Definition

The goal of this study was to compare the environmental impacts of the catalytic methane decomposition process using

https://doi.org/10.1021/acssuschemeng.5c13361
ACS Sustainable Chem. Eng. 2026, 14, 6083−6098

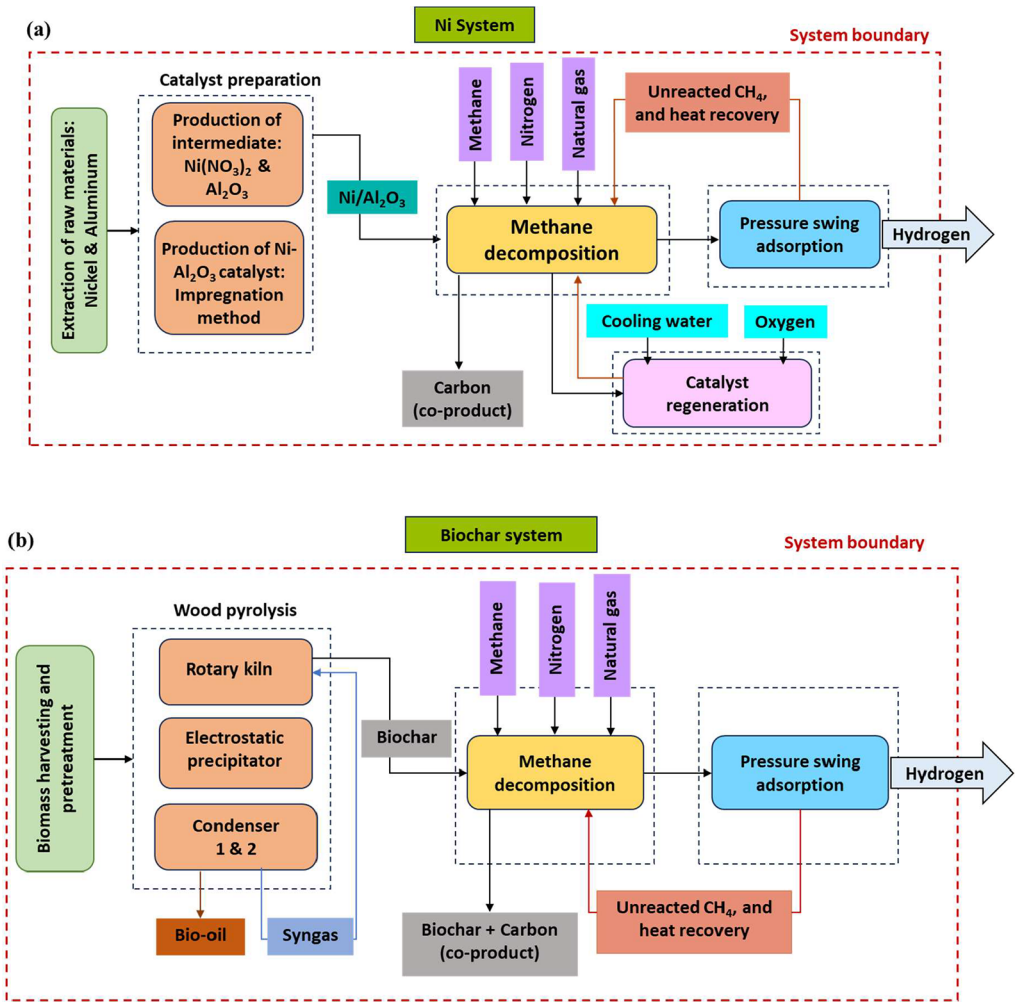

Figure 1. System overview of catalytic methane decomposition using (a) Ni/Al_2O_3 (Ni system) and (b) biochar (biochar system).

Ni/Al_2O_3 and biochar as a catalyst. The functional unit was 1 kg H_2 production at the mill gate. This study adopts a cradle-to-gate approach, starting from raw material extraction to the point where hydrogen exits the production facility, as shown in Figure 1. To improve clarity, we specify the background and foreground systems:

a. Background system: the background system includes all indirect processes required to support the foreground system, which are modeled using the ecoinvent 3.9.1 database. These include (1) raw material supply: nickel and alumina extraction for the Ni system and biomass harvesting and pretreatment for the Biochar system. (2) Energy inputs: natural gas and electricity supply for reactor heating, catalyst preparation, and pressure swing adsorption (PSA) operations, as well as recycling syngas from biochar pyrolysis for heat generation in the Biochar system. (3) Ancillary materials: Other supporting materials such as water, oxygen for Ni catalyst regeneration, and chemicals used in catalyst synthesis.
b. Foreground system: the foreground system represents all direct processes that are actively controlled or influenced during CMD. These processes include (1) catalyst preparation: for the Ni system, this includes the synthesis of the Ni/Al_2O_3 catalyst through the impregnation method, as well as the catalyst regeneration process required due to carbon deposition. For the Biochar system, this includes the pyrolysis of biomass in a rotary kiln to produce biochar, bio-oil, and syngas. (2) Methane decomposition: methane decomposition I considered in a continuous fixed-bed reactor to produce hydrogen and solid carbon. (3) Hydrogen separation: PSA is considered to separate hydrogen from unreacted methane and nitrogen in both catalytic systems.

Overview of the Methane Decomposition Systems and Scenarios

The study evaluated hydrogen production systems, based on other works[19−22] we are assuming a plant lifetime of 30 years with 330 operational days per year for both catalytic systems. Two systems are considered for the catalytic methane decomposition process divided by the catalyst selection. Figure 1 shows the system boundary of both catalytic systems using Ni/Al_2O_3 (a: Ni system) and biochar (b: Biochar system).

Ni system includes raw material extraction and catalyst preparation, methane decomposition, PSA, and catalyst regeneration. Ni system begins with the extraction of raw materials, followed by the production of intermediate (production of nickel(II) nitrate and aluminum oxide) and the Ni/Al_2O_3 catalyst using the impregnation method. Methane and nitrogen are fed into the methane decomposition reactor, producing hydrogen and carbon as a byproduct. Hydrogen, unreacted methane, and carrier nitrogen are then

https://doi.org/10.1021/acssuschemeng.5c13361
ACS Sustainable Chem. Eng. 2026, 14, 6083−6098

Table 1. Comparing Different Ni-Based and Carbon-Based Catalysts Used for the CMD Process

catalysts	reaction temperature (°C)	reaction conversion (%)	gas hourly space velocity (GHSV)	reaction time (h)	feed composition	ref
Ni-Based/Modified Catalysts						
60 wt %Ni/Al_2O_3	650	80	42,000[a]		CH_4:N_2 = 30:70	28
62 wt %Ni/SiO_2·MgO	572	60	24,000[b]	10	CH_4:N_2 = 15:85	29
10NiO/5Al_2O_4	600	100−80	6000[b]	0.08	CH_4:N_2 = 5:90	30
50 wt %Ni 10 wt %Cu/Al_2O_3	675	70	12,000[b]	10	CH_4:N_2 = 30:70	31
50 wt %Ni-5 wt %Cu/SiO_2·MgO	575	85	24,000[b]	5	CH_4:N_2 = 15:85	8
15 wt %Fe-3 wt %Ni/MgO	700	70	5000[b]	3	CH_4:N_2 = 1.5	32
55 wt % Ni/2 wt % MgO·Al_2O_3	600	60	48,000[b]	7	CH_4:N_2 = 15:85	33
Carbon-Based Catalysts						
biochar (activated)	850	21−7	15,000[b]	3	CH_4 = 100	34
biochar	900	51−20	6000[b]	6	CH_4:N_2 = 90:10	12
activated carbon	900	67−17	360[a]	10		35
commercial carbon black	850	12.4	10,000[b]		CH_4 = 100	36
activated biochar	800	94−50	0.1[a]	10	CH_4:N_2 = 50:50	26
biochar (heat treated)	1000	50−12	15,000[b]	4	CH_4:N_2 = 20:80	27
Fe/biochar	850	24.39	5000[b]		CH_4 = 100	4
activated carbon/carbon $black_{1.0}$ (AC/$CB_{1.0}$)	950	33	600[b]	3	CH_4 = 100	37

[a]Unit: h^{-1}. [b]Unit: mL $(g_{cat.}·h)^{-1}$.

processed through PSA to separate and purify the hydrogen. The system also includes a catalyst regeneration step, where the Ni/Al_2O_3 catalyst is restored for reuse, ensuring the efficient continuation of the methane decomposition process.

The biochar CMD system utilizes biochar as a catalyst, emphasizing the use of renewable resources for hydrogen production. The system includes biochar production through pyrolysis, methane decomposition, and PSA. The process begins with biomass harvesting and pretreatment, followed by pyrolysis in a rotary kiln, which produces biochar, bio-oil, and synthesis gas (syngas). The generated syngas is recycled back to the rotary kiln to provide coheat to lower the energy consumption. Methane and nitrogen are introduced into the methane decomposition reactor, where hydrogen and carbon (as a byproduct) are generated. Same as the metal-based catalytic system, hydrogen, unreacted methane, and carrier nitrogen are then processed through pressure swing adsorption to separate and purify the hydrogen. In contrast to the Ni system, the Biochar system does not include a catalyst regeneration unit because carbon deposition on biochar catalyst is desired to enhance the carbon content of biochar (enhanced biochar). The enhanced biochar can be sold as a commodity product to improve the economics of the Biochar system.[23−25]

Table 1 presents reports evaluating different metallic and carbon-based catalysts used in the CMD process. Based on our previous research,[26,27] biochar for its high porosity has shown promising results as a carbon-based catalyst for methane decomposition. For instance, a comparison of the catalytic performance of various materials, including activated biochar (AB), heat-treated biochar (HB), activated carbon (AC), and zeolite, both with and without ruthenium (Ru) doping, showed that Ru-AC and AB had the highest conversion rates at 800 °C. Ru-AC achieved a methane conversion rate of 21%, while AB achieved a significantly higher conversion rate of 51% after a 60 h reaction period.[27] In addition, depositing additional carbon on biochar enhances its carbon content. Therefore, we selected biochar for its properties and market potential as high-value carbon. Additionally, due to the well-established efficacy of Ni-based catalysts, we have chosen Ni/Al_2O_3 for the metal-based category. We aim to provide a clear comparison between these two catalytic systems, highlighting their respective advantages and disadvantages, and contribute valuable insights into the environmental and economic viability of hydrogen production through CMD.

The reaction conditions and performance of two catalysts, Ni/Al_2O_3, and biochar, used in the methane decomposition process and the assumptions considered for the two systems are presented in Table 2. This comparison highlights the differences in operating conditions and efficiencies between the two catalytic systems for hydrogen production through methane decomposition.

Catalyst Testing Protocol and Performance Metrics

The performance of Ni/Al_2O_3 and biochar catalysts was evaluated based on methane conversion rate, catalyst stability over time, and carbon deposition yield, using data from literature (Table 1) and selected assumptions (Table 2). Key metrics and results are summarized below:

Ni/Al_2O_3 Catalyst. Methane decomposition experiments were assumed to be conducted in a continuous fixed-bed reactor under controlled conditions. The reaction temperature was maintained at 650 °C with a GHSV of 42,000 mL/h·g_{cat}, as detailed in Table 2. The methane-to-nitrogen ratio was set at 95:05. Methane conversion rates are typically measured using gas chromatography to quantify methane and hydrogen concentrations in the product stream.[32,27]

https://doi.org/10.1021/acssuschemeng.5c13361
ACS Sustainable Chem. Eng. 2026, 14, 6083−6098

Table 2. Operation Condition of Catalytic Methane Decomposition Using Two Catalytic Systems

catalysts	reaction temperature (°C) (assumption based on Table 1)	reaction conversion (%) (assumption based on Table 1)	catalyst (kg/kg H_2) (calculated in this work)	gas hourly space velocity ($L/h{\cdot}g_{cat}$) (experimental[12,17])	feed composition	feed flow (L/kg H_2)
Ni/Al_2O_3	650	60%	7.5×10^{-03}	42	95%CH_4, balance N_2	11,239,[a] 10,168[b]
biochar	900	35%	5.3×10^{-01}	6	95% CH_4, balance N_2	19,046,[a] 17,232[b]

[a]Total flow. [b]Methane flow.

Biochar Catalyst. Biochar testing was assumed to be conducted under similar conditions in a fixed-bed reactor at 950 °C, with a GHSV of 6000 mL/h·g_{cat} and a methane-to-nitrogen ratio of 95:05 (Table 2). The biochar catalyst was assumed to achieve a methane conversion of 35% (Table 2) and to produce enhanced biochar with increased carbon content, suitable for applications such as carbon black.[6]

Life Cycle Inventory (LCI)

The life-cycle inventory includes all the necessary input and output data needed for our model, allowing us to assess the CMD process systematically at each stage. Inventory data are sourced from the ecoinvent 3.9.1 database, simulation results using SuperPro Designer v13 b3, published papers, and author calculations and are shown in Table S-A1 of the Supporting Information.

Catalyst Preparation. *Ni/Al2O3 Catalyst Preparation.* The impregnation method was selected as the catalyst synthesis method based on the information provided by Akande et al.[38] which includes Ni impregnation on the alumina support, followed by drying at 110 °C for 10 h and calcination at 600 °C for 3 h. Inventory data, including materials, waste, and emissions, are taken from Agarski et al.[39] Due to the frequent deactivation and regeneration of the Ni catalyst in the CMD process, we assume that the methane decomposition was performed for 3 h, followed by catalyst regeneration after each cycle. Throughout 12 cycles, no significant decline in catalytic activity was observed.[40]

Biomass Pyrolysis (Biochar Production). In this process, pine wood chips from the ecoinvent database was used as the feedstock for pyrolysis. The literature indicates that various biomass types; including seaweed,[34] biosolids,[12] Douglas fir,[26] rice husk,[4] poplar[27] bark,[27] and red pine[27] have been employed for biochar production and tested in methane decomposition reactions. Based on our previous work regarding the impact of biomass type on methane conversion, surface acidity was identified as a critical factor that enhances catalyst performance and should be a primary consideration in biochar selection. Consequently, pine wood was chosen for this work due to its suitable surface properties and the availability of reliable inventory data. The energy demand for biomass pyrolysis significantly depends on factors such as pyrolysis temperature, plant capacity, and biomass moisture content.[41,42] The plant capacity was assumed to be 1 t of biochar production per hour. Flue gas is used as a carrier gas instead of nitrogen to make the process more economical and efficient. Biochar was the primary product of this system; however, bio-oil, an aqueous phase, and syngas are also produced during this process. The wood pyrolysis reaction was modeled based on other studies for hardwood,[43] setting the biochar yield to be 20% of the oven-dried feed biomass. Given the commercial use of bio-oil, the economic allocation was considered virtually equal between biochar ($0.4/kg) as the main product and raw bio-oil ($0.4/kg), as a coproduct.[44] The required energy for the cocurrent rotary kiln was produced by natural gas combustion, with synthesis gas (syngas) being recycled back into the system.[45] The fuel/air ratio was maintained at 0.33. The syngas output temperature was set to 250 °C to avoid tar formation. The woody biomass moisture content after drying was kept at 10%. Solid particles are filtered using an electrostatic precipitator (ESP), assuming a filtration efficiency of 95%. Two condensers are used for separating bio-oil and the aqueous phase, with the temperatures set to 95 and 80 °C,

https://doi.org/10.1021/acssuschemeng.5c13361
ACS Sustainable Chem. Eng. 2026, 14, 6083−6098

respectively. In this work, it was assumed that a biochar catalyst bed had a lifetime of 3 h.[27]

Methane Decomposition Process. In this process, fossil-based methane was used as a feedstock, natural gas was utilized as a heating agent for the methane decomposition reactor. A continuous fixed-bed reactor was employed, followed by a gas cyclone for gas−solid separation. It assumed that no emissions or waste were produced in this step, and no side reactions occurred. All inventory data for this process are calculated using simulations performed in the SuperPro Designer model. The simulation models and their corresponding itemized utility consumptions are presented in SuperPro Designer simulations S-B1 to S-B3 and Tables S-B1−S-B3 in Supporting Information B.

Although the overall process layouts of the two pathways are similar, their equipment sizing and energy requirements differ substantially. As shown in Table 2, the biochar system requires 5.3×10^{-01} kg of catalyst per functional unit, compared to only 7.5×10^{-03} kg for the Ni-based system. Owing to the lower intrinsic catalytic activity of biochar, a significantly larger reactor volume (approximately twice that of the Ni system) and a higher operating temperature (900 °C) are required to achieve the same hydrogen production rate. Furthermore, the lower single-pass methane conversion in the biochar system increases the recycle load, imposing a higher energy demand on the PSA unit. As a result, the total electricity consumption of the biochar pathway is approximately double that of the Ni-based system, amounting to 12.07 kW h per functional unit compared to 5.07 kW h for the Ni system (see Tables S-B2 and S-B3 for the detailed energy breakdown). Despite this operational energy penalty, the biochar pathway benefits from a structurally simpler process design. Unlike the Ni-based system, which requires an additional catalyst regeneration step that constitutes a major source of direct CO_2 emissions, the biochar system operates without a regeneration loop. Moreover, the higher yield of solid carbon byproducts further offset the increased energy demand at the system level.

Pressure Swing Adsorption (PSA). In this stage, the mixture of produced gas (hydrogen, unreacted methane, and nitrogen) is fed into the PSA unit to separate hydrogen from the unreacted methane and nitrogen. In this work, it was assumed that the PSA unit included two adsorbent columns with a lifetime of 10 years, which used activated carbon as the adsorbent, although other adsorbents like zeolite and silica gel could be used 45. It was assumed that all unreacted methane and carrier nitrogen are going through heat recovery and recycled back into the system, resulting in a process conversion rate of 99%.

Ni/Al_2O_3 Catalyst Regeneration. It is well-known that any metal catalyst used for methane decomposition will eventually become deactivated due to carbon deposition on the catalyst surface. The catalyst regeneration and separation of carbon materials are significant challenges when using metallic catalysts. It was assumed that 67% of the solid carbon was separated from the Ni catalyst (in the Ni system) by attrition using the mechanisms explained elsewhere.[47,48] The deactivated catalyst was regenerated by burning the carbon deposited during the methane decomposition process. Catalyst regeneration was conducted using the reaction $C + O_2 \rightarrow CO_2$ at 500 °C in the presence of air inside the regenerator reactor, with a 99% reaction conversion.[28] Consequently, CO_2 emissions were considered in this step. According to the literature,[46] 12% catalyst deactivation was observed after 8 regeneration cycles. By extrapolating these findings to the 12 cycles utilized in this study, we estimated a total deactivation range of 18−36%. This corresponds to an average deactivation of approximately 2% per cycle during the regeneration process before the catalyst is reused.

Solid Carbon Byproduct and Physical Allocation. CMD is notable for its CO_x-free hydrogen production. It produces solid carbon, which is both storable and usable. If biomethane is used, this process yields biogenic carbon, contributing to a carbon-negative route.[49] Previous works have shown that the carbon coproduct enhanced the carbon content of the biochar, results indicating a graphite-like pattern.[26,27] Additionally, numerous reports,[30,50−53] have documented the production of carbon nanotubes (CNTs) ($111,000−662,000/Mt), carbon black ($1500/Mt), and graphite ($800−1750/Mt) while using metal-based catalysts. In 2022, the carbon nanomaterials market showed significant diversity in pricing and volume. Lower-priced nanocarbons, ranging from $0.5−10/kg, represented a substantial portion of the market. Meanwhile, high-value carbon products, priced above $100/kg, also demonstrated considerable market presence. This price disparity highlights the wide range of applications and quality levels within the carbon nanomaterials sector, suggesting potential for value addition in carbon-derived materials in the CMD process.[5,54] Therefore, in both Ni and Biochar systems, physical and economic allocation was considered between the hydrogen and the marketable carbon coproduct to use in graphite electrodes.[54]

Life-Cycle Impact Assessment (LCIA)

Impact assessment serves as a crucial step in converting complex inventory analysis data into more accessible information for a broader audience. Specifically, LCIA converts the detailed inputs, outputs, and emissions identified during the inventory analysis into environmental impacts.[33,34,55] This transformation allows for a clearer understanding of the impacts associated with the studied system or product. In this study, environmental impacts are assessed following the TRACI 2.1 method, which considers ten different environmental impact categories, including acidification, carcinogenic, ecotoxicity, eutrophication, fossil fuel depletion, global warming, noncarcinogenic, ozone depletion, respiratory effects, and smog. For all impact categories, TRACI considers two key factors: the quantity of chemical emissions or resource use, and the estimated strength of these environmental (characterization) factors. The strength estimates are derived from the most current models and data available for each impact category. While some categories, such as ozone depletion and global warming, have internationally agreed-upon strength rankings, others rely on chemical and physical models or experimental data. The concept of a large-scale 'hydrogen economy' was proposed primarily as a response to the depletion of fossil resources, with climate change being a secondary consideration.[56] As such, we focus on both fossil fuel depletion and global warming in this study, aiming to address the dual concerns of environmental sustainability and the challenges posed by continued reliance on fossil fuels.

Scenario Analysis

Factors such as limited access to actual plant data, scaling effects, biased assumptions, and differences in local conditions can all influence LCA outcomes. To tackle these issues, we evaluated different scenarios considering different assumptions

https://doi.org/10.1021/acssuschemeng.5c13361
ACS Sustainable Chem. Eng. 2026, 14, 6083−6098

for LCIA, using different resources and ranges of critical parameters.

Impact of Allocation. One of the key advantages of methane decomposition over conventional hydrogen production methods is the simultaneous generation of valuable solid carbon as a byproduct alongside hydrogen.[47] For example, Monolith, a company based in Nebraska, USA, employs methane decomposition to produce hydrogen and solid carbon for carbon black applications. Thus, CMD is notable not only for producing pure hydrogen but also for its potential to generate a high-value coproduct. In this study, we incorporate physical allocation between hydrogen and carbon as coproducts, following the approach of other methane decomposition companies in valorizing both outputs. This physical allocation significantly influences the LCA results, underscoring the importance of applying it correctly. To provide a broader perspective, we also examine an alternative scenario in which carbon is not treated as a commercial coproduct but as a waste to be disposed of (i.e., no value), allowing us to evaluate its effect on the overall outcomes.

Accordingly, we applied economic allocation in our model. As no direct economic calculations were performed in this study, literature-based prices were used to derive the economic allocation factors presented in Table S-A2 in Supporting Information. These factors represent the cost distribution between hydrogen as the primary product and carbon as the coproduct. For example, in the Ni-catalyzed system, 62% of the environmental burden is allocated to hydrogen and 38% to carbon, whereas in the Biochar system, 51% is allocated to hydrogen and 49% to carbon. These economic allocation ratios are based on assumed market prices of $2.12/kg for hydrogen and $0.64/kg for carbon. Furthermore, given the variability of carbon market prices (ranging from 0.44 to 2.21 US$/kg),[53] we evaluated the model using low, base, and high price scenarios (Table S-A3). This approach ensures that our results capture a comprehensive range of potential market impacts.

Using Renewable Resources. From an energy perspective, methane decomposition is a highly heat-intensive process, requiring significant energy to operate. Additionally, the reliance on fossil-based methane as the primary feedstock raises concerns about the long-term sustainability and reliability of this method for hydrogen production. To address these challenges, we explored replacing fossil-based resources with renewable alternatives to evaluate their impact on the process. Specifically, we assessed a scenario where electricity was sourced from grid-connected photovoltaic (PV) power plants and biogenic methane (96% by volume) derived from syngas generated in a wood gasification plant. Data for these renewable resources were obtained from the ecoinvent database.

Gas Hourly Space Velocity (GHSV). One of the most important parameters in process design is the gas hourly space velocity, as it controls the contact time between the catalyst surface and the feed gas, thereby playing a key role in reaction kinetics. For methane decomposition using carbon-based catalysts, the GHSV typically falls within the range of 1−15 L/h·g_{cat},[27] whereas for metal-based catalysts the values are considerably higher, varying from 5−50 L/h·g_{cat}, as shown in Table 1. Previous studies[29−33] have reported that variations in GHSV directly influence methane conversion. Since this process is still under development, we conducted sensitivity analyses by varying the GHSV above and below our baseline values reported in the literature to examine how different assumptions affect system performance. As summarized in Table 3, published data were used to define the GHSV variations, which in turn adjust both the conversion rates and operating temperatures in our model. Although these variations reflect literature-based assumptions rather than optimized conditions, they provide useful insights into how different catalytic systems perform under comparable modeling conditions. For the Ni-based system, we also incorporated catalyst deactivation after each regeneration cycle, which explains why the reported conversion values are lower than those cited in the original references.

Table 3. Sensitivity Analyses Operating Conditions of Catalytic Methane Decomposition Using Two Catalytic Systems

	GHSV (L/h·g_{cat})	temperature (°C)	conversion (%)	ref
Biochar System				
lower	0.6	950	27	37
base case	6	900	35	12
higher	15	1000	25	27
Ni System				
lower	24	572	40	29
base case	42	650	60	28
higher	48	600	40	33

Catalyst Lifetime. The current catalyst designs for CMD remain at the laboratory scale, with the most significant challenge being the loss of catalytic activity. Achieving both high activity and long-term stability simultaneously remains difficult. Presently, most reported solid catalysts exhibit a lifespan of less than 10 h. Over time, carbon accumulation on the catalyst surface during methane decomposition leads to gradual deactivation, requiring either regeneration or replacement of the catalyst after a certain reaction period. In this context, catalyst lifetime plays a critical role in influencing the LCA results, making it essential to assess the model's sensitivity to this parameter. To examine the impact, the model is tested for varying lifetimes of 6×/÷2 h and 12×/÷2 cycles from the base conversion for the Biochar and Ni systems, respectively, to observe differences in the outcomes. Based on various reports, we have selected an average range of catalyst lifetimes for the sensitivity tests.

Ni/Al_2O_3 System Without Regeneration. One of the key distinctions between the two systems modeled in this work is the regeneration process. For the Biochar system, catalyst regeneration is not performed, while in the Ni system catalyst is regenerated to conserve resources and reduce the environmental impact of the system. To evaluate the impact of catalyst regeneration on the overall the Ni system, a sensitivity analysis was conducted to quantify the emissions assuming that the Ni catalyst is not regenerated. This analysis provides valuable insights into the environmental trade-offs associated with catalyst regeneration and its contribution to the system's emissions.

RESULT AND DISSCUSSION

Table 4 presents the LCA results for the production of 1 kg of hydrogen, encompassing various impact categories. The analysis revealed that the Biochar system has a lower environmental impact across all categories. In the subsections below, all data are analyzed and explained in detail. Additionally, to provide broader context regarding noncatalytic

https://doi.org/10.1021/acssuschemeng.5c13361
ACS Sustainable Chem. Eng. 2026, 14, 6083−6098

Table 4. Life Cycle Assessment Results for Cradle-to-Gate Production of 1 kg Hydrogen, Physical Allocation

impact categories	unit	Ni system	biochar system	% change[a]
acidification	kg SO_2 eq	3.86×10^{-2}	2.86×10^{-2}	−25.90
carcinogenic	CTUh	4.01×10^{-7}	5.22×10^{-7}	30.60
ecotoxicity	CTUe	2.02×10^{3}	2.43×10^{3}	20.16
eutrophication	kg N eq	6.15×10^{-2}	6.98×10^{-2}	13.54
fossil fuel depletion	MJ surplus	15.32	11.30	−26.22
global warming	kg CO_2 eq	4.38	3.04	−30.51
noncarcinogenic	CTUh	6.25×10^{-5}	7.51×10^{-5}	20.14
ozone depletion	kg CFC^{-11} eq	1.25×10^{-6}	8.26×10^{-7}	−33.75
respiratory effects	kg $PM^{2.5}$ eq	2.68×10^{-3}	1.94×10^{-3}	−27.63
smog	kg O_3 eq	1.37×10^{-1}	1.63×10^{-1}	19.73

[a]% Differences in impacts relative to the Ni-system: $\left[\frac{I_{\text{biochar}} - I_{\text{Ni}}}{I_{\text{Ni}}} \times 100\right]$.

methane decomposition, we modeled two process configurations based on reported literature data. These reference scenarios are presented in section "Comparison with Non-Catalytic Baseline" and Tables S-A4 and S-A5 of the Supporting Information.

Global Warming (GW) Impact

Global warming impact (often expressed as kg CO_2 eq) is recognized as one of the major global environmental concerns and is subsequently studied in most LCA studies nowadays. Thus, in this work, we focused more on this category. TRACI 2.1 utilizes global warming impact for calculating the potency of greenhouse gases relative to CO_2. As presented in Table 4, the Biochar system, which used biochar as a catalyst, had a lower GW impact of 3.04 kg CO_2 eq, while the Ni system had 4.38 kg CO_2 eq The Biochar system consumed more overall energy but produced less emissions and required fewer raw materials. As mentioned earlier, using a metallic catalyst increases the environmental impact of the system due to the need for the extraction of metals and additional catalyst regeneration steps.

Although the reaction conditions for the Ni system required lower energy, the metallic catalyst preparation and regeneration resulted in a larger contribution to GW impact compared to the Biochar system. According to the global warming contribution bar graph for Biochar and Ni systems shown in Figure 2, the higher GW impact of the Ni system compared to the Biochar system is primarily due to catalyst production and regeneration, which contribute about 40% of emissions. During catalyst regeneration, the system consumes oxygen (produced by an air separation unit) and tap water, while emitting CO_2 as a byproduct. As shown in Figure 2, the contribution of the regeneration step is even greater than that of electricity consumption.

In contrast, while electricity consumption is the dominant factor in the Biochar system, its overall GW impact remains lower than the Ni system. This is due to the higher operation temperature and lower conversion of the carbonaceous catalytic system in the CMD process. Other factors, such as methane consumption, show similar contributions as expected in both systems. Based on these outcomes, improving the electricity efficiency of the Biochar system could make it more sustainable and environmentally friendly.

Compared to SMR, CMD has lower CO_2 emission.[19,47] Oni et al.[19] compared SMR, ATR, and natural gas decomposition (NGD) hydrogen production methods and reported that producing 1 kg of H_2 without considering carbon capture effects resulted in 11.35, 11.01, and 4.89 kg CO_2 eq/kg H_2, respectively. Their results for natural gas decomposition showed close alignment with our results. However, the difference in emissions could be attributed to the selection of a different metallic catalyst (they used an iron ore catalyst), as well as variations in catalyst lifetime and reaction conditions. Additionally, different electricity grids played an important role in emission calculations.[57] Electricity generation differs across regions and countries, depending on the mix of fossil and renewable sources, and this composition strongly influences the life cycle performance of a product. For instance, Vu et al.,[58] reported varying emission levels under different electricity supply configurations: 3.23 kg CO_2e/kg H_2 for dispatchable renewable energy (RE), 3.81 kg CO_2e/kg H_2 for variable RE, and 6.14 kg CO_2e/kg H_2 for Powerlink electricity. In another study,[47] researchers compared the GHG emissions of methane decomposition using carbon and Fe_3O_4/Al_2O_3 as catalysts. Their results showed that both systems with 70% conversion had 0.22 kg CO_2/Nm_3 H_2 (2.44 kg CO_2/kg H_2) and 0.26 kg CO_2/Nm_3 H_2 (2.89 kg CO_2/kg H_2) when metal catalysts are used. Furthermore, Mio et al.[59] conducted an LCA comparing hydrogen production methods: green hydrogen (electrolysis using photovoltaic power), grid hydrogen (electrolysis with grid electricity), gray hydrogen (steam reforming of natural gas), and blue hydrogen (gray hydrogen with carbon capture using hot potassium carbonate). Their findings showed emissions of 4.23, 5.27, 12.6, and 23.5 kg CO_2/kg H_2 for

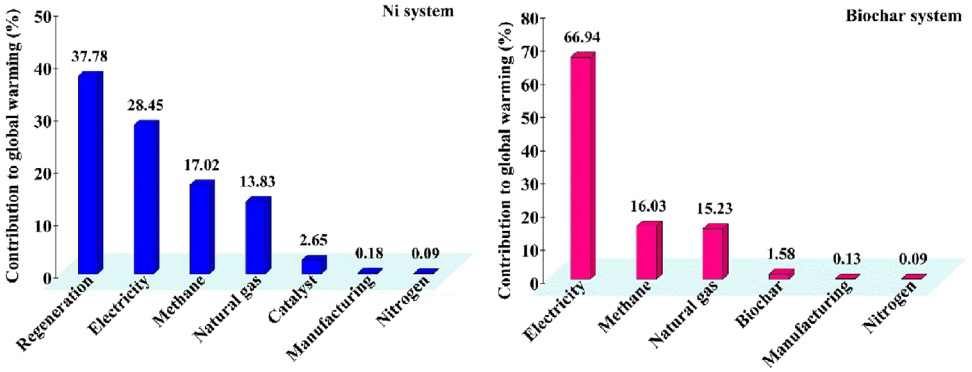

Figure 2. Percent contribution to global warming impact from cradle-to-gate for two catalytic hydrogen production systems, physical allocation (note: "manufacturing" refers to the production of steel and other materials used to fabricate equipment for process plants).

https://doi.org/10.1021/acssuschemeng.5c13361
ACS Sustainable Chem. Eng. 2026, 14, 6083−6098

green, blue, gray, and grid hydrogen, respectively. These results highlight green hydrogen as the most sustainable option, followed by blue hydrogen. Figure 3 provides a comparative

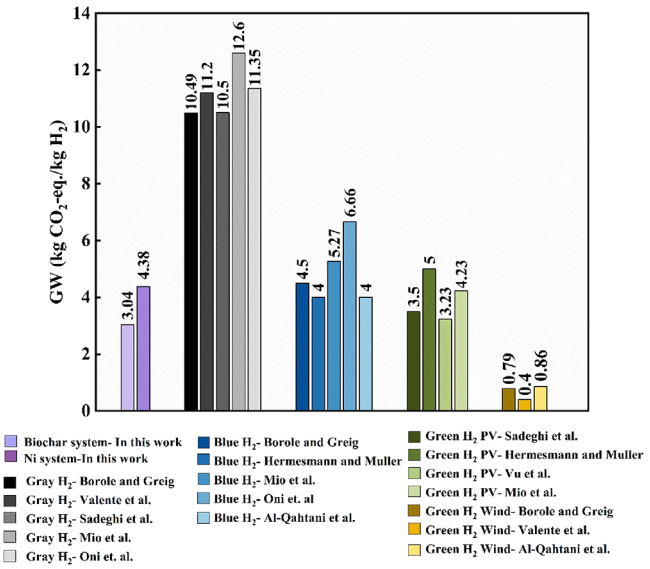

Figure 3. Comparison of GW impact results from this study with gray, blue, and green H_2 results from other studies.[19,58−64]

analysis of the global warming impact associated with different hydrogen production pathways, including gray, blue, and green hydrogen from the literature, alongside the results from this study for biochar-based and Ni-catalyzed methane decomposition systems. From the Figure 3, it is evident that gray hydrogen production methods, which rely on natural gas steam reforming without carbon capture, exhibit the highest GW impact values, often exceeding 10 kg CO_2 eq/kg H_2. This underscores the significant environmental burden associated with conventional hydrogen production. The blue hydrogen pathways, which incorporate carbon capture and storage (CCS) to mitigate CO_2 emissions, demonstrate a marked reduction in GW impact compared to gray hydrogen. However, the emissions remain substantial, with values typically ranging from 4 to 7 kg CO_2 eq/kg H_2, depending on the efficiency of the carbon capture technology and the specific feedstock used. Green hydrogen, produced via electrolysis using renewable energy sources such as solar (PV) and wind, presents the lowest GW impact, often below 2 kg CO_2 eq/kg H_2, making it the most environmentally friendly option. However, the high cost and scalability challenges of renewable-powered electrolysis remain key barriers to widespread adoption. In comparison, the biochar-based hydrogen system proposed in this work demonstrates a notable environmental advantage over gray hydrogen and is comparable to blue hydrogen. The GW impact of the Biochar system falls within the range of green hydrogen, highlighting the environmental advantages of using biochar as a catalyst. This advantage is attributed to the sustainable origin of biochar, which facilitates carbon sequestration and significantly reduces the net carbon footprint relative to conventional hydrogen production pathways. This comparison is crucial as it positions the environmental impacts of CMD within the wider spectrum of hydrogen production technologies, further justifying the potential of CMD, particularly when integrated with renewable energy sources and catalysts like sustainably sourced biochar.

Fossil Fuel Depletion (FFD)

The increasing demand for fossil fuels may lead to a greater impact on resource depletion in the future.[57] From the data in Table 4, for Ni system and Biochar system, the FFD values are 15.32 and 11.30 MJ surplus, respectively. As depicted in Figure 4, in both systems, methane used as a feedstock contributed the most to this category, with the Ni system showing 81.63% and the Biochar system showing 72.83%. Utilizing methane from nonfossil-based resources could help mitigate the FFD effect, as discussed in section Using Renewable Resources.

In the Biochar system, natural gas and electricity have a higher contribution to FFD compared to the Ni system. This is primarily due to the higher operating temperature of the Biochar system, which increases its natural gas consumption. However, in the Ni system, catalyst production has a significantly higher contribution to FFD compared to the Biochar system.

Electricity consumption also contributed to FFD, though to a lesser extent (7.37% for the Ni system and 16.43% for the Biochar system). The impact of electricity on FFD is lower compared to the direct use of natural gas and methane, partly because approximately 80% of U.S. electricity is generated from fossil sources, while the remaining is generated from renewable sources.[65]

Similar to the GW results, catalyst production, and regeneration in the Ni system are the factors differentiating the environmental impacts in this category. Addressing these factors, particularly by sourcing methane from renewable

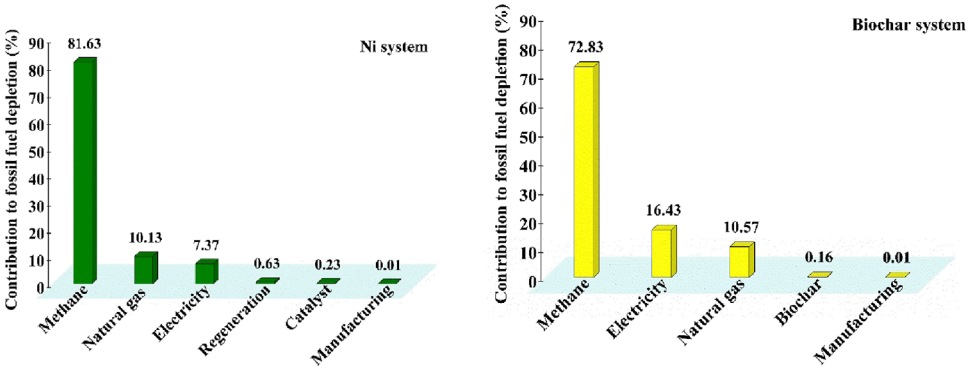

Figure 4. Contribution to fossil fuel depletion from cradle-to-gate for two catalytic hydrogen production systems, physical allocation (note: "manufacturing" refers to the production of steel and other materials used to fabricate equipment for processing plants).

https://doi.org/10.1021/acssuschemeng.5c13361
ACS Sustainable Chem. Eng. 2026, 14, 6083−6098

resources, such as biomethane, and optimizing process conditions, could enhance the sustainability of hydrogen production processes.

Biomethane can be produced through three primary pathways: anaerobic digestion, thermal gasification of biomass, and synthesis from renewable hydrogen and carbon dioxide. The feasibility of anaerobic digestion is liable to the local availability of suitable waste streams as feedstock, which can vary significantly by region.[66]

In terms of scale, both existing and planned synthetic fuel production facilities are still limited in number and capacity, suggesting that large-scale biomethane production is unlikely to occur before 2030. According to estimates from the German Biomass Research Centre (DBFZ), a total of 48−50 billion cubic meters of biomethane could be produced by 2030, of which 18−20 billion cubic meters may be upgraded for injection into the natural gas grid or utilized as a transportation fuel.[66]

According to the U.S. Energy Information Administration (EIA), total natural gas consumption in 2024 was approximately 3310 billion cubic meters. In parallel, the United States has made notable progress in implementing manure-based anaerobic digestion systems, which play a key role in reducing methane emissions from livestock waste. As of June 2024, about 400 systems were in operation, collectively mitigating an estimated 95.7 million metric tons of CO_2 eq emissions between 2000 and 2023. In 2023 alone, these systems produced around 3.29 million MWh of energy, highlighting the significant potential of biomethane as a sustainable and low-carbon energy source.[67]

Other Categories

Other impact categories of the TRACI impact assessment method include acidification, eutrophication, ozone depletion, photochemical smog formation, and human health (carcinogenic, noncarcinogenic, and ecotoxicity) impacts. The comparison reveals a clear trade-off in performance between the two systems across these categories.

As shown in Table 4, the Biochar system exhibits higher impacts than the Ni system regarding eutrophication, human health, and smog. To understand these results, it is important to note that eutrophication refers to the impacts of excess nutrient elements exceeding natural levels, which can shift species composition and alter biomass production.[57] Similarly, human health impacts refer to the potential of a compound or physical agent to cause harmful effects on the environment and organisms,[68] while ecotoxicological stress from chemical emissions is a globally recognized threat to biodiversity. The primary driver for the Biochar system's higher impact in these categories is the significant electricity demand of the PSA process (see Supporting Information B). Because a portion of the U.S. electricity grid is generated from hard coal, electricity usage accounts for the largest share of emissions in these specific categories. Specifically, electricity contributes approximately 80−90% of the Biochar system's impact and 60−70% of the Ni system's impact for eutrophication and human health. Consequently, the Ni system outperforms the Biochar system in these areas primarily due to its lower electrical load.The results for photochemical smog formation, however, show a different distribution of contributors. Smog formation is mainly caused by combustion processes[69] and is further influenced by sunlight incidence, which varies by geographical location.[57] While electricity remains a factor, the Biochar system is heavily impacted by biomass pyrolysis (30%) and natural gas combustion (15%), with electricity contributing 43%. The Ni system, which does not require biomass pyrolysis and has a lower electricity load, therefore demonstrates better performance in minimizing smog formation. Finally, natural gas combustion and electricity were identified as the main contributors to the acidification impact category. Impacts from ozone depletion were found to be negligible, remaining in the range of 10^{-7} as ozone-depleting components are very limited in the atmosphere.

Sensitivity Analysis

Impact of Allocation. One of the key points that made catalytic methane decomposition particularly attractive and promising for scale-up is the production of high-value solid carbon, in addition to CO_x-free hydrogen. As shown in Figure 5 and Table 5, the environmental impacts increased by about

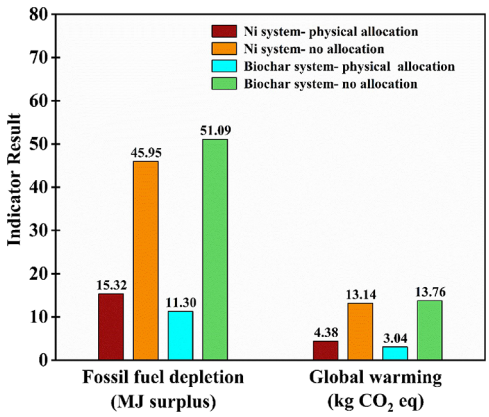

Figure 5. Sensitivity of allocation on GW impact and FFD for two catalytic hydrogen production systems, per 1 kg H_2.

Table 5. Life Cycle Assessment Results for the Cradle-to-Gate Catalytic Production of 1 kg Hydrogen, No Allocation

impact categories	unit	Ni system	biochar system	% change[a]
acidification	kg SO_2 eq	1.16×10^{-1}	1.29×10^{-1}	11.65
carcinogenic	CTUh	1.20×10^{-6}	2.36×10^{-6}	96.20
ecotoxicity	CTUe	6.06×10^{3}	11×10^{3}	81.06
eutrophication	kg N eq	1.84×10^{-1}	3.16×10^{-1}	71.11
fossil fuel depletion	MJ surplus	45.95	51.09	11.17
global warming	kg CO_2 eq	13.14	13.76	4.74
noncarcinogenic	CTUh	1.87×10^{-4}	3.39×10^{-4}	81.04
ozone depletion	kg CFC^{-11} eq	3.74×10^{-6}	3.73×10^{-6}	−0.18
respiratory effects	kg $PM^{2.5}$ eq	8.04×10^{-3}	8.77×10^{-3}	9.09
smog	kg O_3 eq	4.10×10^{-1}	7.42×10^{-1}	80.90

[a]% Differences in impacts relative to the Ni system $\left[\frac{I_{\text{biochar}} - I_{\text{Ni}}}{I_{\text{Ni}}} \times 100\right]$.

70% for the Ni system and 80% for the Biochar system across different categories when physical allocation is not applied in the LCA. Figure 5 illustrates the sensitivity of the physical allocation parameter on GW and FFD for two systems. For the Ni system, the FFD rises from 15.32 MJ surplus to 45.95 MJ surplus, and the GW impact increases from 4.38 kg CO_2 eq to 13.14 kg CO_2 eq Similarly, for the Biochar system, the FFD escalates from 11.30 MJ surplus to 51.09 MJ surplus, and the GW impact jumps from 3.04 kg CO_2 eq to 13.76 kg CO_2 eq.

https://doi.org/10.1021/acssuschemeng.5c13361
ACS Sustainable Chem. Eng. 2026, 14, 6083−6098

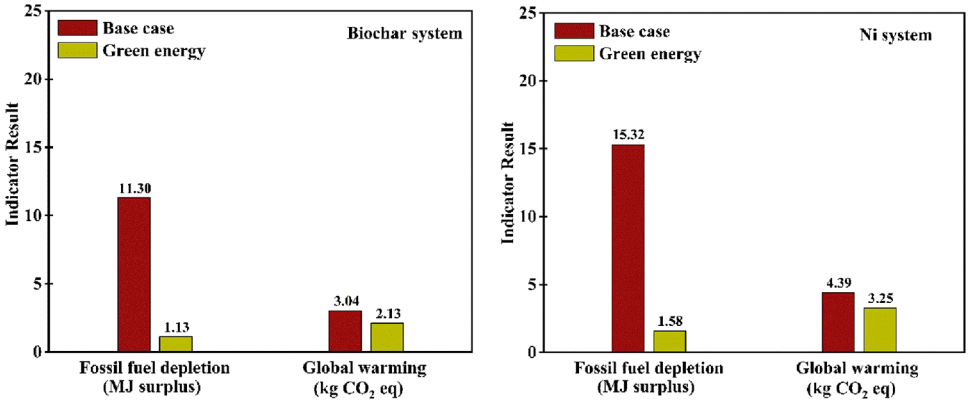

Figure 6. Sensitivity of renewable energy use on GW and FFD for two catalytic hydrogen production systems, per 1 kg H_2 (cradle-to-gate), physical allocation.

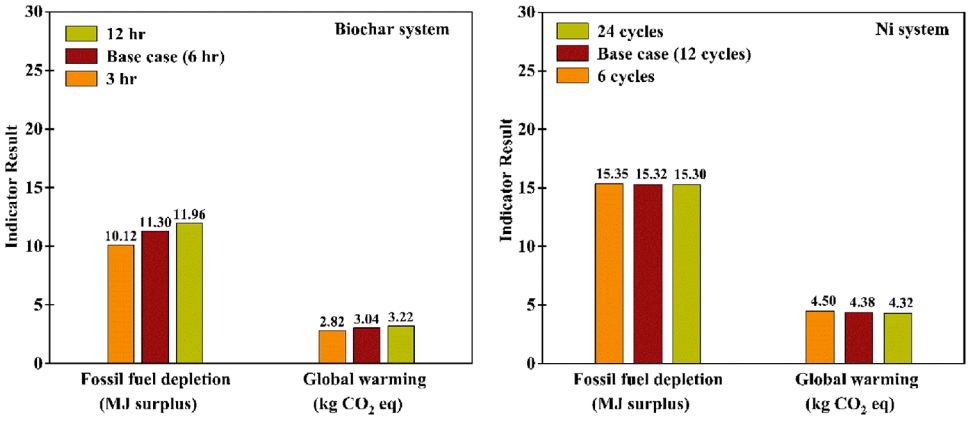

Figure 7. Sensitivity of catalyst lifetime on GW and FFD for two catalytic hydrogen production systems from cradle-to-gate, per 1 kg H_2, physical allocation.

The economic allocation results are presented in Table S-A4 of the Supporting Information. These findings highlight the critical role of allocation in reducing the life-cycle environmental impacts of both systems, underscoring its importance in LCA. Notably, because the Biochar system yields 50% more carbon product than the Ni-based system, applying physical or economic allocation leads to lower environmental impacts for the biochar pathway. In addition, it has been reported that the utilization of carbon in different industries makes hydrogen production from methane decomposition economically competitive, even compared with conventional technologies.[5,49] Given the variability in carbon market prices, we performed a sensitivity analysis across a range of potential values. The results (Figure S-A1) demonstrate that, at a constant hydrogen price, the carbon price plays a significant role in the environmental performance. specifically, higher carbon prices can reduce the environmental impact by approximately 50%, while lower market values could increase the GW impact and FFD by 15−20%.

It is important to note that without the commercial usage of the carbon produced during the CMD process, it would not be able to economically compete with other conventional methods of hydrogen production. Rather than focusing only on environmental factors, selling carbon byproducts can significantly enhance plant revenue and overall profitability. According to a techno-economic analysis,[19] hydrogen production costs are \$1.22, \$1.23, and \$2.12 per kg H_2 for SMR, ATR, and NGD, respectively, assuming a natural gas price of \$1.96/GJ. Methane decomposition results in the highest hydrogen production cost. However, these analyses did not account for the potential revenue from selling carbon byproducts. In contrast, another study[54] calculated a hydrogen production cost of \$2.28 per kg H_2 at a natural gas price of \$4.84/GJ, incorporating a carbon credit of \$0.64 per kg H_2. This inclusion substantially reduced the overall hydrogen cost, demonstrating that carbon byproduct sales can enhance the economic viability of methane decomposition for hydrogen production.

Using Renewable Resources. Figure 6 illustrates the impact of using methane produced from wood and solar energy as a power source on the FFD and GW of both catalytic systems. The reference scenario, which uses fossil-based methane, natural gas, and conventional electricity, shows an FFD of 11.30 MJ surplus for the Biochar system and 15.32 MJ surplus for the Ni system. In contrast, when green energy parameters are applied, the FFD dramatically decreases to 1.13 and 1.58 MJ surplus for the Biochar and Ni systems, respectively, indicating a substantial reduction in direct fossil fuel usage. Similarly, the GW impact shows about a 30 and 26% reduction for Biochar and Ni systems, respectively, reflecting the benefits of using renewable energy sources.

As highlighted in Figure 4, fossil-based methane, natural gas, and electricity contribute significantly to the FFD in reference scenarios. Replacing these with renewable alternatives reduces FFD by up to 90%. In terms of GW, electricity had the most substantial impact on the Biochar system. Although the

https://doi.org/10.1021/acssuschemeng.5c13361
ACS Sustainable Chem. Eng. 2026, 14, 6083−6098

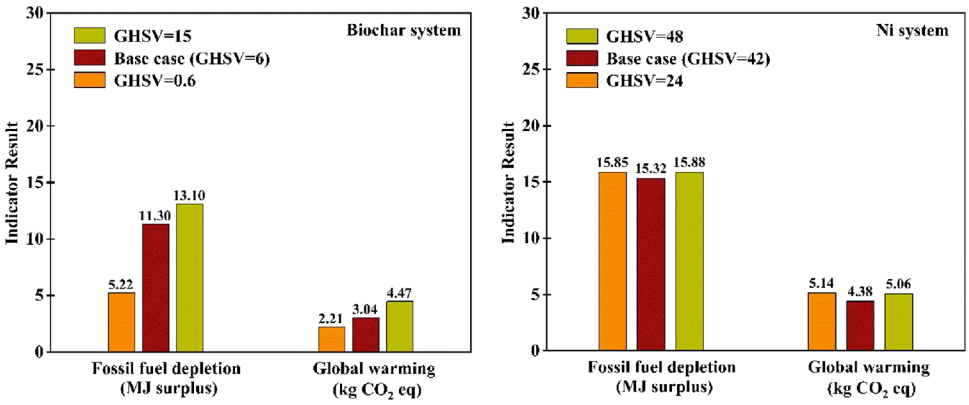

Figure 8. Sensitivity of GW and FFD to GHSV variation in two catalytic hydrogen production systems from cradle-to-gate, per 1 kg H_2, mass allocation.

decrease in GW is less than that in FFD, the transition to clean (green) energy still results in a significant reduction. Previous studies have reported a reduction of 82.1 g CO_2 eq/km in life cycle emissions when using biomethane instead of fossil fuels, corresponding to a 95% decrease in emissions.[70] These findings suggest that utilizing sustainably sourced renewable resources such as synthetic methane and solar energy and incorporating biochar as a catalyst can lower the environmental impacts of hydrogen production. However, maximizing efficiency in clean power production is critical to avoid a high carbon footprint. This underscores that efficiency is a governing factor for the environmental impact of both thermal and clean energy systems.[71]

Catalyst Lifetime. In all catalytic processes, catalyst lifetime plays an important role in process efficiency. Catalyst lifetime affected raw material extraction, energy usage for catalyst synthesis, transportation, and plant shutdown/overhaul expenses. All these factors are reduced when the catalyst's lifetime is extended. In this work, we calculated the GW impact for producing 1 kg of Ni/Al_2O_3 and biochar, which are 46.27 kg CO_2 eq and 1.01 kg CO_2 eq, respectively. The outcomes revealed that, even under a lower lifetime assumption, using biochar catalysts remains advantageous, as producing biochar from woody biomass is far less environmentally harmful than manufacturing metal-based catalysts. According to the outcomes shown in Figure 7, there is no significant change in GW and FFD by varying the Ni system lifetime in the CMD process (due to the catalyst regeneration). However, catalyst lifetime has a greater impact in the Biochar system. Since biochar use also generates carbon as a valuable coproduct, it can be regarded as a revenue stream for the system. Nevertheless, to reduce maintenance costs, it is more appropriate to consider the average catalyst lifetime.

Gas Hourly Space Velocity. In this section, the LCA model is applied to evaluate the effect of varying GHSV from the baseline values in both systems (Figure 8). Changes in reaction parameters influence several energy-related factors, including electricity demand, heat requirements from natural gas, catalyst consumption, and CO_2 emissions. As GHSV increases, the contact time between the feed gas and catalyst surface decreases. Figure 8 presents the sensitivity results for both systems under different GHSV assumptions. However, due to limitations in the published data, we were unable to simultaneously fix both the conversion and reaction temperature and therefore treated GHSV as the only variable. To maintain consistency, we selected conditions that were as close as possible to our baseline case. In the Biochar system, increasing GHSV results in higher environmental impacts. At lower GHSV, a larger catalyst bed is required, which increases the overall amount of biochar used. By the end of the reaction cycle, this produces not only more spent biochar but also greater amounts of carbon byproduct, resulting in a larger system credit. For example, the case with GHSV = 0.6 L/h·g_{cat} shows the best environmental performance, but it requires one more kg of catalyst and about 40% larger reactor compared to the base case, which limits scalability. In practice, higher GHSV values, such as those in the baseline case, are more common in carbon-based CMD designs. For the Ni system, variations in GHSV have only a minor influence on GW and FFD impacts. Unlike the Biochar system, the metal catalyst cannot be credited as a carbon coproduct, so the small increases in FFD and GW at nonoptimal GHSV values are primarily due to reduced conversion. Consistent with literature reports, the baseline case of 42 L/h·g_{cat} delivers the best performance.[50,72] Other studies further confirm that Ni-based catalysts perform comparably at around 600 °C, with GHSV variation exerting little effect on overall outcomes.[72,73]

The optimization of CMD reactions ultimately relies on the careful adjustment of multiple interdependent factors, including catalyst composition, preparation methods, reactor configuration, and feed conditions. Literature highlights several promising strategies for enhancing performance. For example, Ni−Cu bimetallic systems have demonstrated high catalytic activity and stability when optimized for metal loading.[8] Advanced synthesis techniques, such as impregnation using the ethylenediaminetetraacetic acid method, improve active metal dispersion and surface area, extending catalyst lifetimes.[72] Moreover, statistical optimization approaches, such as the Taguchi design, allow for systematic identification of optimal synthesis parameters (e.g., pH, aging temperature, surfactant type) to maximize conversion and stability.[8] Building on these findings, future research should integrate these optimization strategies into practical CMD systems to achieve improved efficiency and scalability.

Ni/Al_2O_3 System without Regeneration. Catalytic methane decomposition has been studied for over a century, but its commercialization remains hindered by significant challenges. Catalyst design is still at the laboratory stage, with rapid deactivation caused by issues such as coking (carbon deposition), poisoning, sintering, and mechanical degradation. Most solid catalysts demonstrate limited lifespans, typically less than 10 h, due to carbon coproduct accumulation that blocks

https://doi.org/10.1021/acssuschemeng.5c13361
ACS Sustainable Chem. Eng. 2026, 14, 6083−6098

active sites and reduces efficiency.[7,14] While catalyst regeneration is often proposed to address deactivation, it introduces secondary emissions, such as CO and CO_2, which might have a negative impact on CMD's environmental benefits. To assess the impact of avoiding catalyst regeneration in the Ni/Al_2O_3 system, a sensitivity analysis was conducted to quantify emissions under the assumption that the catalyst is not regenerated.[7,14] The results (Figure 9) indicate that regenerating the Ni/Al_2O_3 catalyst has negligible impact on environmental performance of the system. Catalyst regeneration produces CO_x gases, which is contrary to the purpose of the catalytic methane decomposition process, namely, hydrogen production without CO_x emissions. Although the Biochar system operates at a higher temperature than the Ni system, its overall environmental performance is improved due to different energy-material trade-offs. The Ni system requires periodic catalyst regeneration, which adds material and energy burdens without improving carbon yield or reducing emissions. In contrast, the Biochar system avoids regeneration; while its higher operating temperature increases electricity demand, this is offset by the use of a renewable catalyst and higher carbon yield, resulting in a lower overall environmental impact.

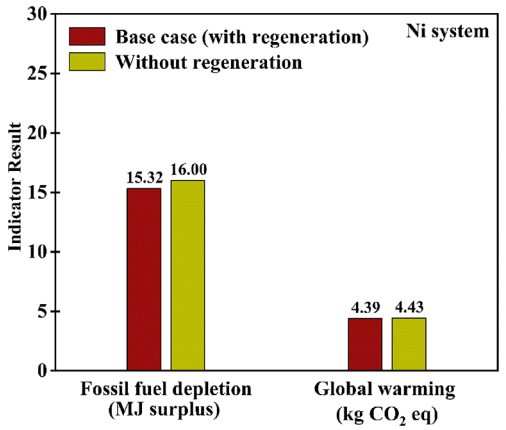

Figure 9. Sensitivity of GW and FFD to catalyst regeneration of the Ni system from cradle-to-gate, per 1 kg H_2, mass allocation.

FUTURE PERSPECTIVE AND OUTLOOK

In recent years, significant research efforts and pilot-scale developments have focused on hydrogen production coupled with the generation of value-added solid carbon via methane decomposition. The use of catalysts in this process plays a crucial role in lowering the reaction temperature, which in turn reduces energy consumption, mitigates material degradation, and enhances overall process safety. Furthermore, catalytic systems offer greater control over the morphology and quality of the produced solid carbon. In the present study, a fixed-bed reactor configuration was adopted, as most available experimental data in the literature are based on this reactor type.[73] However, it is well documented that in catalytic methane decomposition, carbon deposition occurs preferentially on the active sites of solid catalysts, leading to catalyst encapsulation and progressive deactivation.[73,74] In fixed-bed reactors, this phenomenon results in increased pressure drop and, ultimately, blockage of the gas flow, severely limiting the feasibility of continuous operation and large-scale industrial application.[74]

To address these challenges, the fluidized-bed reactor (FBR) has emerged as a promising alternative. Fluidized beds provide superior heat and mass transfer characteristics compared to packed beds and are particularly well suited for multiphase reaction systems such as CMD.[75] More importantly, they enable continuous feeding of fresh catalysts and simultaneous withdrawal of spent catalysts along with the deposited carbon, thereby reducing carbon accumulation and allowing for stable, continuous operation.[73−76] Extending the present work to incorporate fluidized-bed reactor design would therefore be a valuable direction for future research, enabling systematic evaluation of how reactor configuration influences process performance and scalability.

Among the few technologies capable of operating both with and without catalysts are plasma- and microwave-assisted systems, in which carbon deposition can occur on plasma arcs or reactor surfaces even in the absence of a solid catalyst.[75,77] Plasma-based methane decomposition has demonstrated notable progress toward industrial implementation, with commercial-scale production of carbon black and hydrogen already reported. Plasma and microwave plasma reactors also offer a high degree of operational flexibility.[75,77] Noncatalytic plasma pyrolysis typically requires extremely high temperatures, on the order of 2100 °C, to achieve methane conversions approaching 94%.[75] In contrast, hybrid plasma-catalytic systems can operate at substantially lower temperatures. For example, laboratory-scale studies at Tomsk have combined a plasma torch with a downstream catalytic stage using nickel-based catalysts, achieving approximately 80% methane conversion at around 1000 °C.[75] These findings indicate that integrating catalysts into plasma-assisted processes may significantly reduce energy demand while maintaining high conversion levels.

Accordingly, a promising avenue for future research would be the simulation and comparative assessment of plasma-assisted methane decomposition with and without catalysts, with particular emphasis on catalyst type, operating temperature, and their combined impact on hydrogen yield, energy efficiency, and carbon product characteristics.

Finally, for contextual completeness, it is noted that this study employs pure methane as the feedstock and does not explicitly model the formation, separation, or utilization of light hydrocarbon side products. If natural gas were used as the feed and high-temperature operation (>850 °C) were considered, minor quantities of species such as ethylene, acetylene, and CO could form.[77] In practical process designs, such components are typically routed to hydrogen purification off-gas streams and utilized as process fuel rather than flared. This discussion is intended to provide perspective for future studies and does not affect the system boundaries or results presented in this work.

CONCLUSIONS

This study provides a comprehensive life cycle assessment comparing the life-cycle environmental impacts of using metal-based (Ni/Al_2O_3) and carbon-based (biochar) catalysts for catalytic methane decomposition from cradle-to-gate to produce hydrogen. Our findings indicate that biochar catalyst present a better environmental option, with lower global warming impact (3.04 kg CO_2 eq for biochar vs 4.38 kg CO_2 eq for Ni/Al_2O_3) and fossil fuel depletion potential (11.30 MJ surplus for biochar vs 15.32 MJ surplus for Ni/Al_2O_3). This advantage is largely due to the absence of the need for catalyst

https://doi.org/10.1021/acssuschemeng.5c13361
ACS Sustainable Chem. Eng. 2026, 14, 6083−6098

regeneration in the biochar case and the market value of the high-value carbon-added biochar produced at the end of the CMD process. The study revealed that the catalyst regeneration process in the Ni/Al_2O_3 system has 37.78% contribution to its GW, producing more CO_2 emissions and requiring more raw materials. Sensitivity analyses demonstrated that improving reaction parameters like GHSV, conversion rate, temperature, and especially incorporating renewable energy sources, such as synthetic (biogenic) methane and solar energy, can significantly reduce the environmental footprint of the CMD process. Key findings include a 30 and 26% reduction in GW for Biochar and Ni systems, respectively, with renewable energy use. Overall, this research highlights the importance of selecting appropriate catalysts to minimize environmental impacts in hydrogen production to mitigate climate change, a critical societal need. The results contribute valuable knowledge to the field, promoting the adoption of sustainable practices and guiding future advancements in CMD technology. By demonstrating the advantages of biochar catalyst, this study supports the broader goal of achieving sustainable and better environmental performing hydrogen production methods.

■ ASSOCIATED CONTENT

Supporting Information

The Supporting Information is available free of charge at https://pubs.acs.org/doi/10.1021/acssuschemeng.5c13361.

Detailed inventory data and economic allocation results (PDF)

Detailed SuperPro designer simulation modeling and energy consumption breakdown (XLSX)

■ AUTHOR INFORMATION

Corresponding Author

Hossein Jahromi − *Biosystems Engineering Department, Auburn University, Auburn, Alabama 36849, United States; Center for Bioenergy and Bioproducts, Auburn University, Auburn, Alabama 36849, United States;* orcid.org/0009-0001-5270-2261; Email: hossein.jahromi@auburn.edu

Authors

Raziyeh Jokar − *Biosystems Engineering Department, Auburn University, Auburn, Alabama 36849, United States*

Ashish Manandhar − *Department of Environmental Engineering and Earth Sciences, Clemson University, Clemson, South Carolina 29634, United States; Food, Agricultural and Biological Engineering Department, Ohio State University, Wooster, Ohio 44691, United States*

Sushil Adhikari − *Biosystems Engineering Department, Auburn University, Auburn, Alabama 36849, United States; Center for Bioenergy and Bioproducts, Auburn University, Auburn, Alabama 36849, United States;* orcid.org/0000-0002-6539-6822

Prakash Nepal − *USDA Forest Service, Forest Products Laboratory, Madison, Wisconsin 53726, United States*

Richard Bergman − *USDA Forest Service, Forest Products Laboratory, Madison, Wisconsin 53726, United States; Department of Forest and Wildlife Ecology, University of Wisconsin-Madison, Madison, Wisconsin 53706, United States;* orcid.org/0000-0003-1798-1717

Naveenkumar Rajendiran − *USDA Forest Service, Forest Products Laboratory, Madison, Wisconsin 53726, United States; Biological Systems Engineering Department, University of Wisconsin-Madison, Madison, Wisconsin 53706, United States*

Ajay Shah − *Food, Agricultural and Biological Engineering Department, Ohio State University, Wooster, Ohio 44691, United States*

Complete contact information is available at: https://pubs.acs.org/10.1021/acssuschemeng.5c13361

Notes

The authors declare no competing financial interest.

■ ACKNOWLEDGMENTS

The authors would like to thank the U.S. Endowment for Forestry Communities for their assistance in funding this study under Grant No. 22-00374. As some authors of this paper are employees of the U.S. Department of Agriculture Forest Service, we emphasize that the findings and conclusions in this report are those of the author(s) and should not be construed to represent any official USDA or U.S. Government determination or policy. Any use of trade, firm, or product names is for descriptive purposes only and does not imply endorsement by the U.S. government.

■ REFERENCES

(1) *Hydrogen production to increase to 110 Mt per year by 2030, study says*. https://www.offshore-energy.biz/hydrogen-production-to-increase-to-110-mt-per-year-by-2030-study-says/ (accessed September 2024).

(2) Azizimehr, B.; Armaghani, T.; Ghasemiasl, R.; Kaabi Nejadian, A.; Javadi, M. A. A comprehensive review of recent developments in hydrogen production methods using a new parameter. *Int. J. Hydrogen Energy* **2024**, *72*, 716−729.

(3) Jokar, R.; Alavi, S. M.; Rezaei, M.; Akbari, E. CO preferential oxidation in H_2-rich stream over the CuO-MnOx mixed oxide catalysts prepared by a facile mechanochemical preparation method. *Int. J. Hydrogen Energy* **2023**, *48*, 24833−24844.

(4) Feng, D.; Wang, J.; Wang, S.; Sun, S.; Shang, Q.; Zhao, Y. Effect of biochar support on the catalytic performance of Fe-based catalysts for CH4 cracking. *Fuel Process. Technol.* **2023**, *247*, No. 107794.

(5) Farhana, K.; Mahamude, A. S.; Kadirgama, K. Comparing hydrogen fuel cost of production from various sources-a competitive analysis. *Energy Convers. Manage.* **2024**, *302*, No. 118088.

(6) Keipi, T.; Tolvanen, H.; Konttinen, J. Economic analysis of hydrogen production by methane thermal decomposition: Comparison to competing technologies. *Energy Convers. Manage.* **2018**, *159*, 264−273.

(7) Fan, Z.; Weng, W.; Zhou, J.; Gu, D.; Xiao, W. Catalytic decomposition of methane to produce hydrogen: A review. *J. Energy Chem.* **2021**, *58*, 415−430.

(8) Karimi, S.; Meshkani, F.; Rezaei, M.; Rastegarpanah, A. The influence of promoters on the catalytic behavior of the Ni/SiO2.MgO catalysts for thermocatalytic decomposition of methane reaction. *Fuel* **2024**, *372*, No. 131945.

(9) Rastegarpanah, A.; Rezaei, M.; Meshkani, F.; Dai, H.; Arandiyan, H. Thermocatalytic decomposition of methane over mesoporous Ni/$xMgO{\cdot}Al_2O_3$ nanocatalysts. *Int. J. Hydrogen Energy* **2018**, *43*, 15112−15123.

(10) Ibrahim, A. A.; Ahmed, H.; Fakeeha, A. H.; Abasaeed, A. E.; Al-Fatesh, A. S.; Osman, A. I. Iron catalysts enhanced by ultrasound for methane decomposition and hydrogen generation. *Int. J. Hydrogen Energy* **2025**, *137*, 851−860.

(11) Salib, C. Q.; Perez-Lopez, O. W. Hydrogen production by methane decomposition over Cu-Ni-Al-LDH: Influence of Ni/Cu ratio and catalyst activation. *Fuel* **2024**, *364*, No. 131120.

(12) Patel, S.; Kundu, S.; Halder, P.; Marzbali, M. H.; Chiang, K.; Surapaneni, A.; Shah, K. Production of hydrogen by catalytic methane decomposition using biochar and activated char produced from biosolids pyrolysis. *Int. J. Hydrogen Energy* **2020**, *45*, 29978−29992.
(13) Li, D.; Dong, H.; Song, G.; Du, Q.; Kawi, S.; Gao, J. Hydrogen and Carbon Nanofiber Coproduction by Methane Decomposition over Ni/Diatomite Catalysts. *ACS Sustainable Chem. Eng.* **2025**, *13*, 3554−3566.
(14) Abbas, H. F.; Wan Daud, W. M. A. Hydrogen production by methane decomposition: A review. *Int. J. Hydrogen Energy* **2010**, *35*, 1160−1190.
(15) International Organization for Standardization. *Environmental Management − Life Cycle Assessment − Requirements and Guidelines; ISO 14044:2006*; ISO: Geneva, Switzerland, 2006.
(16) International Organization for Standardization. *Environmental Management − Life Cycle Assessment − Principles and Framework; ISO 14040:1997*; ISO: Geneva, Switzerland, 1997.
(17) Timmerberg, S.; Kaltschmitt, M.; Finkbeiner, M. Hydrogen and hydrogen-derived fuels through methane decomposition of natural gas − GHG emissions and costs. *Energy Convers. Manage.: X* **2020**, *7*, No. 100043.
(18) Dufour, J.; Serrano, D. P.; Gálvez, J. L.; Moreno, J.; González, A. Hydrogen production from fossil fuels: Life cycle assessment of technologies with low greenhouse gas emissions. *Energy Fuels* **2011**, *25*, 2194−2202.
(19) Oni, A. O.; Anaya, K.; Giwa, T.; Di Lullo, G.; Kumar, A. Comparative assessment of blue hydrogen from steam methane reforming, autothermal reforming, and natural gas decomposition technologies for natural gas-producing regions. *Energy Convers. Manage.* **2022**, *254*, No. 115245.
(20) Mohamed, A. M. O.; Al-Ghamdi, S. G.; Bicer, Y. Life cycle assessment of clean ammonia synthesis from thermo-catalytic solar cracking of liquefied natural gas. *Int. J. Hydrogen Energy* **2021**, *46*, 38551−38562.
(21) Khojasteh Salkuyeh, Y.; Saville, B. A.; MacLean, H. L. Techno-economic analysis and life cycle assessment of hydrogen production from natural gas using current and emerging technologies. *Int. J. Hydrogen Energy* **2017**, *42*, 18894−18909.
(22) Zhang, J.; Ling, B.; He, Y.; Zhu, Y.; Wang, Z. Life cycle assessment of three types of hydrogen production methods using solar energy. *Int. J. Hydrogen Energy* **2022**, *47*, 14158−14168.
(23) Gu, H.; Bergman, R.; Anderson, N.; Alanya-Rosenbaum, S. Life-cycle assessment of activated carbon from woody biomass. *Wood Fiber Sci.* **2018**, *50*, 229−243.
(24) Bergman, R.; Gu, H.; Alanya-Rosenbaum, S.; Liang, S. *Comparative life-cycle assessment of biochar activated carbon and synthesis gas electricity with commercially available alternatives; General Technical Report FPL-GTR-270*; U.S. Department of Agriculture, Forest Service, Forest Products Laboratory: Madison, WI, 2019.
(25) Anderson, N.; Gu, H.; Bergman, R. Comparison of Novel Biochars and Steam Activated Carbon from Mixed Conifer Mill Residues. *Energies* **2021**, *14*, 8472.
(26) Harun, K.; Adhikari, S.; Jahromi, H. Hydrogen production: via thermocatalytic decomposition of methane using carbon-based catalysts. *RSC Adv.* **2020**, *10*, 40882−40893.
(27) Jokar, R.; Jahromi, H.; Bhattrai, A.; Adhikari, S. Biocarbon-catalyzed methane decomposition towards clean hydrogen and enhanced biocarbon production. *Int. J. Hydrogen Energy* **2024**, *70*, 105−117.
(28) Gao, B.; Wang, I. W.; Ren, L.; Haines, T.; Hu, J. Catalytic Performance and Reproducibility of Ni/Al2O3$ and Co/Al_2O_3 Mesoporous Aerogel Catalysts for Methane Decomposition. *Ind. Eng. Chem. Res.* **2019**, *58*, 798−807.
(29) Karimi, S.; Meshkani, F.; Rezaei, M.; Rastegarpanah, A. Thermocatalytic decomposition of CH_4 over Ni/SiO_2.MgO catalysts prepared via surfactant-assisted urea precipitation method. *Fuel* **2021**, *284*, No. 118866.
(30) Zeng, Y. C.; Law, Z. X.; Tsai, D. H. Combined methane cracking for H_2 production with CO_2 utilization for catalyst regeneration using dual functional nanostructured particles. *ACS Sustainable Chem. Eng.* **2024**, *12*, 12200−12215.
(31) Bayat, N.; Rezaei, M.; Meshkani, F. Methane dissociation to CO_2-free hydrogen and carbon nanofiber over Ni-Cu/Al_2O_3 catalysts. *Fuel* **2017**, *195*, 88−96.
(32) Al-Fatesh, A.-S.; Barama, S.; Ibrahim, A.-A.; Barama, A.; Khan, W.-U.; Fakeeha, A. Study of Methane Decomposition on Fe/MgO-Based Catalyst Modified by Ni, Co, and Mn Additives. *Chem. Eng. Commun.* **2017**, *204*, 739−749.
(33) Rastegarpanah, A.; Rezaei, M.; Meshkani, F.; Dai, H.; Arandiyan, H. Thermocatalytic decomposition of methane over mesoporous Ni/xMgO.Al_2O_3 nanocatalysts. *Int. J. Hydrogen Energy* **2018**, *43*, 15112−15123.
(34) Zhao, S.; Zhang, L.; Hu, H.; Jin, L. Catalytic decomposition of methane over enteromorpha prolifera-based hierarchical porous biochar. *Int. J. Hydrogen Energy* **2023**, *48*, 3328−3339.
(35) Nishii, H.; Miyamoto, D.; Umeda, Y.; Hamaguchi, H.; Suzuki, M.; Tanimoto, T.; Harigai, T.; Takikawa, H.; Suda, Y. Catalytic activity of several carbons with different structures for methane decomposition and by-produced carbons. *Appl. Surf. Sci.* **2019**, *473*, 291−297.
(36) Zhou, N.; Zhao, D.; Su, Q.; Li, Q.; Zha, W.; Feng, S. Catalytic performance of modified carbon black on methane decomposition for hydrogen production. *RSC Adv.* **2024**, *14*, 15656−15663.
(37) Yang, L.; Liu, S.; Xu, H.; Liu, F.; Zhang, J. Study on the mechanism of constructing structure defects on surface of activated carbon with carbon black to promote hydrogen production by thermal-decomposition of methane. *Fuel* **2024**, *361*, No. 130758.
(38) Akande, A. J.; Idem, R. O.; Dalai, A. K. Synthesis, characterization and performance evaluation of Ni/Al2O3 catalysts for reforming of crude ethanol for hydrogen production. *Appl. Catal., A* **2005**, *287*, 159−175.
(39) Agarski, B.; Nikolić, V.; Kamberović, Ž.; Anđić, Z.; Kosec, B.; Budak, I. Comparative life cycle assessment of Ni-based catalyst synthesis processes. *J. Cleaner Prod.* **2017**, *162*, 7−15.
(40) Choudhary, T. V.; Goodman, D. W. Methane decomposition: Production of hydrogen and carbon filaments. In *Catalysis*; RSC, 2006; pp 164−183.
(41) Sahoo, K.; Upadhyay, A.; Runge, T.; Bergman, R.; Puettmann, M.; Bilek, E. Life-cycle assessment and techno-economic analysis of biochar produced from forest residues using portable systems. *Int. J. Life Cycle Assess.* **2021**, *26*, 189−213.
(42) Bergman, R.; Gu, H.; Page-Dumroese, D. S.; Anderson, N. *Life Cycle Analysis of Biochar [Chapter 3]*. Cambridge University Press: Cambridge: U.K., 2016; pp 46−69.
(43) Ranzi, E.; Cuoci, A.; Faravelli, T.; Frassoldati, A.; Migliavacca, G.; Pierucci, S.; Sommariva, S. Chemical kinetics of biomass pyrolysis. *Energy Fuels* **2008**, *22*, 4292−4300.
(44) Inayat, A.; Ahmed, A.; Tariq, R.; Waris, A.; Jamil, F.; Ahmed, S. F.; Ghenai, C.; Park, Y. K. Techno-Economical Evaluation of Bio-Oil Production via Biomass Fast Pyrolysis Process: A Review. *Front. Energy Res.* **2022**, *9*, No. 770355.
(45) Luberti, M.; Ahn, H. Review of Polybed pressure swing adsorption for hydrogen purification. *Int. J. Hydrogen Energy* **2022**, *47*, 10911−10933.
(46) Fakeeha, A. H.; Barama, S.; Ibrahim, A. A.; Al-Otaibi, R. L.; Barama, A.; Abasaeed, A. E.; Al-Fatesh, A. S. In situ regeneration of alumina-supported Cobalt−iron catalysts for hydrogen production by catalytic methane decomposition. *Catalysts* **2018**, *8*, 567.
(47) Dufour, J.; Gálvez, J. L.; Serrano, D. P.; Moreno, J.; Martínez, G. Life cycle assessment of hydrogen production by methane decomposition using carbonaceous catalysts. *Int. J. Hydrogen Energy* **2010**, *35*, 1205−1212.
(48) Shah, N.; Ma, S.; Wang, Y.; Huffman, G. P. Semi-continuous hydrogen production from catalytic methane decomposition using a fluidized-bed reactor. *Int. J. Hydrogen Energy* **2007**, *32*, 3315−3319.
(49) Mirkarimi, S. M. R.; Bensaid, S.; Negro, V.; Chiaramonti, D. Review of methane cracking over carbon-based catalyst for energy and fuels. *Renewable Sustainable Energy Rev.* **2023**, *187*, No. 113747.

https://doi.org/10.1021/acssuschemeng.5c13361
ACS Sustainable Chem. Eng. 2026, 14, 6083−6098

(50) Pourdelan, H.; Alavi, S. M.; Rezaei, M.; Akbari, E.; Klyamkin, S. Thermocatalytic Decomposition of Methane Over NiO−MgO Catalysts Synthesized by the Mechanochemical Method. *Catal. Lett.* **2023**, *153*, 733−742.
(51) Mahmoodzade, E.; Meshkani, F.; Rezaei, M.; Rastegarpanah, A. Preparation and improvement of nickel catalyst supported ordered mesoporous spherical silica for thermocatalytic decomposition of methane. *J. Energy Inst.* **2020**, *93*, 2488−2496.
(52) Hondo, E.; Gani, T. Z. H.; Kosari, M.; Xi, S.; Bella; Ashok, J.; Tan, J. Y.; Wang, T.; Bian, H.; Lim, K. H.; Chen, L.; Chang, J.; Borgna, A.; Kawi, S. Unveiling the Roles of Precursor Structure and Controlled Sintering on Ni-Phyllosilicate-Derived Catalysts for Low-Temperature Methane Decomposition. *ACS Sustainable Chem. Eng.* **2023**, *11*, 8786−8799.
(53) Hantoko, D.; Khan, W. U.; Osman, A. I.; Nasr, M.; Rashwan, A. K.; Gambo, Y.; Al Shoaibi, A.; Chandrasekar, S.; Hossain, M. M. Carbon−neutral hydrogen production by catalytic methane decomposition: a review. *Environ. Chem. Lett.* **2024**, *22*, 1623−1663.
(54) Lane, J. M.; Spath, P. L. *Technoeconomic Analysis of the Thermocatalytic Decomposition of Natural Gas; NREL/TP-570−29653*; National Renewable Energy Laboratory: Golden, CO, 2001.
(55) Shah, A.; Baral, N. R.; Manandhar, A. Technoeconomic Analysis and Life Cycle Assessment of Bioenergy Systems. In *Advances in Bioenergy*; Elsevier: Amsterdam, 2016; vol *1*, pp 189−247.
(56) Weidner, T.; Tulus, V.; Guillén-Gosálbez, G. Environmental sustainability assessment of large-scale hydrogen production using prospective life cycle analysis. *Int. J. Hydrogen Energy* **2023**, *48*, 8310−8327.
(57) Manandhar, A.; Shah, A. Life cycle assessment of feedstock supply systems for cellulosic biorefineries using corn stover transported in conventional bale and densified pellet formats. *J. Cleaner Prod.* **2017**, *166*, 601−614.
(58) Vu, H.; Chang, D. Life cycle global warming impact of a green hydrogen supply chain: A case study of Australia to South Korea. *Appl. Energy* **2025**, *397*, No. 126339.
(59) Mio, A.; Barbera, E.; Massi Pavan, A.; Bertucco, A.; Fermeglia, M. Sustainability analysis of hydrogen production processes. *Int. J. Hydrogen Energy* **2024**, *54*, 540−553.
(60) Hermesmann, M.; Müller, T. E. Green, Turquoise, Blue, or Grey? Environmentally friendly Hydrogen Production in Transforming Energy Systems. *Prog. Energy Combust. Sci.* **2022**, *90*, No. 100996.
(61) Al-Qahtani, A.; Parkinson, B.; Hellgardt, K.; Shah, N.; Guillen-Gosalbez, G. Uncovering the true cost of hydrogen production routes using life cycle monetisation. *Appl. Energy* **2021**, *281*, No. 115958.
(62) Valente, A.; Iribarren, D.; Dufour, J. Prospective carbon footprint comparison of hydrogen options. *Sci. Total Environ.* **2020**, *728*, No. 138212.
(63) Sadeghi, S.; Ghandehariun, S.; Rosen, M. A. Comparative economic and life cycle assessment of solar-based hydrogen production for oil and gas industries. *Energy* **2020**, *208*, No. 118347.
(64) Borole, A. P.; Greig, A. L. Life-cycle assessment and systems analysis of hydrogen production. In *Biohydrogen*, 2nd edition; Pandey, A., Ed.; Elsevier: Amsterdam, 2019; pp 485−512.
(65) U.S. Environmental Protection Agency. *About the U.S. electricity system and its impact on the environment*. https://www.epa.gov/energy/about-us-electricity-system-and-its-impact-environment (accessed December 2024).
(66) Heyne, S.; Bokinge, P. *Global production of bio-methane and synthetic fuels − overview; Report 2019:305*; Energiforsk: Stockholm, Sweden, 2019.
(67) U.S. Environmental Protection Agency. *AgSTAR Data and Trends*. https://www.epa.gov/agstar/agstar-data-and-trends (accessed December 2024).
(68) Roy, K.; Kar, S. In Silico Models for Ecotoxicity of Pharmaceuticals. In *Ecotoxicity In Vitro, In Vivo and In Silico Models*; Springer: New York, NY, 2016; pp 237−304.
(69) Thomas, N. *Comparative Assessment of the Potential Impact of Pesticides Used in the Catchment of Lake Geneva*; Agroscope Reckenholz-Tänikon Research Station ART: Zurich, Switzerland, 2008.
(70) Ravindran, J. K.; Fagg, D. P.; Coelho, M. C. Current production routes and life cycle analysis of "Green Energy-Dense Fuels" from biogas: A comprehensive review. *Appl. Energy* **2025**, *402*, No. 126832.
(71) Li, Z.; Li, J.; Cao, Z.; Hu, K.; Ao, R.; Li, J.; Li, J.; Wang, X.; Zhang, S.; Yan, Y.; Li, M. Spatiotemporal carbon footprints of electricity production and consumption in China. *Cell Rep. Sustain.* **2025**, *2* (11), No. 100466.
(72) Karimi, S.; Meshkani, F.; Rezaei, M.; Rastegarpanah, A. Development of a novel method to synthesize Ni/SiO_2.MgO catalysts using EDTA as a chelating agent for the methane decomposition process. *Powder Technol.* **2024**, *443*, No. 119896.
(73) Qian, J. X.; Chen, T. W.; Enakonda, L. R.; Liu, D. B.; Mignani, G.; Basset, J. M.; Zhou, L. Methane Decomposition to Produce COx-Free Hydrogen and Nano-Carbon over Metal Catalysts: A Review. *Int. J. Hydrogen Energy* **2020**, *45*, 7981−8001.
(74) Patlolla, S. R.; Katsu, K.; Sharafian, A.; Wei, K.; Herrera, O. E.; Mérida, W. A Review of Methane Pyrolysis Technologies for Hydrogen Production. *Renewable Sustainable Energy Rev.* **2023**, *181*, No. 113323.
(75) Schneider, S.; Bajohr, S.; Graf, F.; Kolb, T. State of the Art of Hydrogen Production via Pyrolysis of Natural Gas. *ChemBioEng. Rev.* **2020**, *7*, 150−158.
(76) Pathak, S.; McFarland, E. Iron Catalyzed Methane Pyrolysis in a Stratified Fluidized Bed Reactor. *Energy Fuels* **2024**, *38*, 12576−12585.
(77) Di Liddo, L.; Cepeda, F.; Saegh, G.; Salakhi, M.; Thomson, M. J. Comparative Analysis of Methane and Natural Gas Pyrolysis for Low-GHG Hydrogen Production. *Int. J. Hydrogen Energy* **2024**, *84*, 146−154.

https://doi.org/10.1021/acssuschemeng.5c13361
ACS Sustainable Chem. Eng. 2026, 14, 6083−6098